Saudi Pharmaceutical Journal (2015) **23**, 528–540

King Saud University

Saudi Pharmaceutical Journal

www.ksu.edu.sa
www.sciencedirect.com

ORIGINAL ARTICLE

Design, optimization and evaluation of glipizide solid self-nanoemulsifying drug delivery for enhanced solubility and dissolution

Rajendra Narayan Dash [a], Mohammed Habibuddin [b,*], Touseef Humaira [b], Devi Ramesh [c]

[a] *Alliance Institute of Advanced Pharmaceutical & Health Sciences, Plot No. 64, Survey No. 145, Sardar Patel Nagar, Kukatpally, Hyderabad 500 072, Telangana, India*
[b] *Adept Pharma and Bioscience Excellence Private Limited, Corporate Office: 10-3-561/3/A/102, Vijayanagar Colony, Hyderabad 500057, Telangana, India*
[c] *Government Polytechnic for Women, Gujarathipeta, Srikakulam, Andhra Pradesh, India*

Received 29 December 2014; accepted 28 January 2015
Available online 19 February 2015

KEYWORDS

Central composite design;
SNEDDS;
Nanoemulsion;
Solubility enhancement;
Dissolution enhancement

Abstract A solid self-nanoemulsifying drug-delivery system (solid SNEDDS) has been explored to improve the solubility and dissolution profile of glipizide. SNEDDS preconcentrate was systematically optimized using a circumscribed central composite design by varying Captex 355 (Oil), Solutol HS15 (Surfactant) and Imwitor 988 (Co-surfactant). The optimized SNEDDS preconcentrate consisted of Captex 355 (30% w/w), Solutol HS15 (45% w/w) and Imwitor 988 (25% w/w). The saturation solubility (*SS*) of glipizide in optimized SNEDDS preconcentrate was found to be 45.12 ± 1.36 mg/ml, indicating an improvement (1367 times) of glipizide solubility as compared to its aqueous solubility (0.033 ± 0.0021 mg/ml). At 90% *SS*, glipizide was loaded to the optimized SNEDDS. *In-vitro* dilution of liquid SNEDDS resulted in a nanoemulsion with a mean droplet size of 29.4 nm. TEM studies of diluted liquid SNEDDS confirmed the uniform shape and size of the globules. The liquid SNEDDS was adsorbed onto calcium carbonate and talc to form solid SNEDDS. PXRD, DSC, and SEM results indicated that, the presence of glipizide as an amorphous and as a molecular dispersion state within solid SNEDDS. Glipizide dissolution improved

Abbreviations: solid SNEDDS, solid self-nanoemulsifying drug delivery system; *SS*, saturation solubility; DR_{15min}, percentage drug release in 15 minutes; LCT, long chain triglycerides; MCT, medium chain triglycerides.

* Corresponding author. Tel./fax: +91 4066103388.
E-mail address: drhabib21@gmail.com (H. Mohammed).

Peer review under responsibility of King Saud University.

Production and hosting by Elsevier

http://dx.doi.org/10.1016/j.jsps.2015.01.024

significantly ($p < 0.001$) from the solid SNEDDS (~100% in 15 min) as compared to the pure drug (18.37%) and commercial product (65.82) respectively.

1. Introduction

Glipizide: 1-Cyclohexyl-3-{4-[2-(5-methylpyrazine-2-carboxamido) ethyl] benzene sulphonyl} urea is an antidiabetic. It is given orally for the treatment of type II diabetes mellitus. Glipizide acts to lower blood glucose by stimulating the release of pancreatic β cell (Sweetman, 2009). Glipizide, a weak acid ($pK_a = 5.9$) is practically insoluble in water (Wilson et al., 2004). Owing to its poor solubility, several formulation approaches have been investigated, including cyclodextrin complex (Gan et al., 2002; Huang et al., 2013; Nie et al., 2011; Shivakumar et al., 2007; Zhang et al., 2008), solid dispersion (Isaac et al., 2013), nanosuspension (Mahesh et al., 2014), bionanocomposites (Kushare and Gattani, 2013), co-solvent assisted solubilization (Seedher and Kanojia, 2009) and microparticles (Madhusudhan et al., 2010) to improve solubility of glipizide.

Self-nanoemulsifying drug-delivery systems (SNEDDS) have emerged as an effective delivery system due to their proven ability to enhance bioavailability of lipophilic drugs (Singh et al., 2013). SNEDDS is a thermodynamically stable isotropic mixture of oil, surfactant, co-surfactant and drug that form a spontaneous oil-in-water nanoemulsion with a droplet size less than 100 nm when introduced into an aqueous medium under gentle agitation (Bali et al., 2011).

Several potential advantages of SNEDDS include their ability to present drug in a solubilized form inside the gastrointestinal (GI) lumen, thus providing greater interfacial area for drug absorption, providing greater chemical and enzymatic stability, inhibiting P-glycoprotein (p-gp) mediated drug efflux, enhancing lymphatic transport (Date et al., 2010; Seo et al., 2013).

Components of SNEDDS and their concentrations have profound effect upon droplet size of the formed nanoemulsion which may affect its *in-vitro* and *in-vivo* performance (Hu et al., 2012). However, such formulations often developed and optimized using a trial-and-error approach by varying one-factor-at-a-time keeping rest factors constant. This univariate approach is time-consuming and requires a larger number of experiments to describe the effect of excipients (oil, surfactant and co-surfactant) on the physical properties of the SNEDDS and frequently fails to project the true optimal composition because interactions between factors were not considered (Pund et al., 2014). For understanding the multi-factorial relationship between formulation factors and product quality usually requires the use of multivariate approach, such as statistical design of experiment (DOE) (Wu et al., 2011). Systematic optimization of pharmaceutical product using DOE requires fewer experimental runs and tends to reveal (any) synergism or interaction among factors. Which in turn leads to yield a robust formulation with advantages of economics in terms of time, money and development efforts (Singh et al., 2013).

Moreover, it is worthy to convert conventional liquid SNEDDS to a solid dosage form (solid SNEDDS) having high stability, better transportability, simple and cost effective manufacturing, and above all, the improved therapeutic success owing to better patient compliance (Balakrishnan et al., 2009; Hu et al., 2012). Thus, the present research work aim at developing a solid SNEEDS of glipizide by systematically optimizing the SNEDDS preconcentrate that would generate a nanoemulsion on dilution. The generation of a nanoemulsion could provide a large interfacial surface area for drug solubilization leading to an enhanced solubility and dissolution of glipizide.

2. Materials and methods

2.1. Materials

Pharmaceutical grade of glipizide was a generous gift from Alembic Ltd., Vadodara, India. Abitec Corp., Janesville, USA, supplied EP/NF grade of medium chain tri-glycerides (Captex® 300, and Captex® 355) and medium chain mono-glycerides (Capmul® MCM,). EP grades of poly-glycol mono and di-esters of 12-hydroxy stearic acid (Solutol® HS15) and polyethylene glycol-40 hydrogenated castor oil (Cremophor® RH40); provided by BASF SE, Ludwigshafen, Germany. EP grade of medium chain tri-glycerides (Labrafac lipophile™ WL 1349, Labrafac™ PG) and PEG-8 glyceryl caprylate (Labrasol®) were supplied by Gattefosse Corp., Saint-Priest, France. EP grades of medium chain tri-glycerides (Miglyol® 812 N) and medium chain mono-glycerides (Imwitor® 988) were supplied by Sasol, GmbH Germany. Tween® 80, Coconut oil, Castor oil, Olive oil, and Polyethylene glycol 400 (PEG 400) were purchased from Himedia Lab. Private Ltd., Mumbai, India. Capsugel Health Care Ltd., Mumbai, India, supplied size "1" hard gelatin capsule shell. 18 MΩ Water (HPLC grade) obtained in-house from a Direct Q-3 UV water purification system (Millipore India Pvt. Ltd., Bengaluru, India).

2.2. Analytical methodology

A reversed phase HPLC method was developed in-house to quantify glipizide in samples obtained from solubility and dissolution studies. The analysis was performed on the Perkin Elmer HPLC system (Series 200) at a temperature of 30 ± 2 °C. The column used (Luna C8, 100 × 4.6 mm, 3 µm) was from Phenomenex®, CA, USA, while the mobile phase was acetonitrile–potassium dihydrogen orthophosphate buffer (pH 4.5; 20 mM) (35:65, v/v). Mobile phase flow rate, detection wavelength and injection volume were 0.8 ml/min, 226 nm and 20 µl respectively. The method was linear ($r^2 = 0.999$) in the concentration range of 0.05–70 µg/ml.

The inter-day and intra-day precision was within the acceptable range of less than 2%.

2.3. Determination of glipizide solubility in oils, optimized SNEDDS preconcentrate and water

Solubility of glipizide determined using the shake flask method. An excess of glipizide was added to vials containing two ml of each medium chain triglyceride (MCT)/synthetic oils (Captex 300, Captex 355, Labrafac lipophile WL1349, Labrafac PG and Miglyol 812 N); long chain triglycerides (LCT) (Coconut oil, Olive oil and Castor oil) and optimized SNEDDS (a mixture of oil, surfactant and co-surfactant). The vials stirred in water bath at 37 ± 0.5 °C for 7 days to attain equilibrium. Similarly, an excess amount of glipizide was added to 10 ml of water (HPLC) and processed as above. All the samples were centrifuged at 5000 rpm for 15 min (RM-12C, Remi-instruments, Mumbai, India) and analyzed for glipizide content by HPLC.

2.4. Screening of surfactants and co-surfactant for emulsifying ability

Surfactant and co-surfactants were selected based upon their ability to emulsify rather than to solubilize the drug (Basalious et al., 2010). Surfactants and Co-surfactants were screened in accordance with the method described by Date and Nagarsenker, 2007 with minor modification. For surfactant screening, 500 mg of each surfactant (Cremophor RH40, Solutol HS15, Labrasol, Cremophor EL and Tween 80) was mixed with 500 mg of oil (selected from solubility study). The mixture was gently heated at 40 °C to homogenize the components. Each mixture (0.1 g) was reconstituted with 50 ml of water (HPLC) in a volumetric flask. The resulting emulsions were visually observed for emulsion formation by noting the number of flask inversion. Percentage transmittance (at 638.2 nm) (Date and Nagarsenker, 2007; Gupta et al., 2011) and turbidity were measured by UV–Vis spectrophotometer (T80 + , PG Instrument, UK) and Digital Nephlo-turbidity meter (132, Systronics, India) respectively using water (HPLC) as blank.

For Co-surfactant screening, 100 mg of each co-surfactant (Imwitor 988, Capmul MCM, Capmul PG8 and PEG 400) was mixed with 200 mg of a surfactant (selected from surfactant screening) at 1:2 ratios. 300 mg of oil was added to the above mixture of surfactant and co-surfactants at 1:1 ratio. The mixture gently heated at 40 °C to homogenize the components and diluted 500 times with water (HPLC). The formed emulsions were accessed for different parameters as mentioned under surfactant screening.

2.5. Ternary phase diagram

To identify the region of nanoemulsion, a ternary phase diagram was plotted for the selected oil, surfactant and co-surfactant, each representing an apex of a triangle. A series of mixtures (2 g each) with varying oil, surfactant and co-surfactant were prepared. The levels of oil, surfactant and co-surfactant were varied from 10 to 80, 10 to 80 and 10 to 50 parts by weight respectively. For any mixture, the sum of oil, surfactant and co-surfactant was 100%. 100 mg of each mixture was added to 20 ml water (HPLC) and agitated gently at 50 rpm using a magnetic stirrer (2MLH, Remi, Mumbai, India). The generated emulsion having a clear or slightly bluish in appearance was considered as the nanoemulsion (Basalious et al., 2010).

2.6. Optimization of SNEDDS preconcentrate using experimental design

A central composite design (CCD) was employed for the optimization of SNEDDS by varying its components/factor such as Captex 355 ($X1$), Solutol HS15 ($X2$), and Imwitor 988 ($X3$). The factors were varied between 20–60 parts by weight of $X1$, 20–60 parts by weight of $X2$ and 10–30 parts by weight of $X3$. The experimental plan was designed using Minitab® version 16 (Minitab, Inc. UK). Twenty formulations (2 g each) with six central points (run order 3, 5, 11, 14, 15 and 17) were prepared by mixing various portions of oil, surfactant and co-surfactant as recommended by the experimental plan (Table 1). Each formulation was diluted with HPLC water (500 times) and assessed for responses such as mean droplet size (nm) ($Y1$), turbidity (NTU) ($Y2$), and percentage transmittance ($Y3$) (Nazzal and Khan, 2002; Pund et al., 2014; Rahman et al., 2012). The optimization's goal was kept to minimize $Y1$ (< 50 nm), $Y2$ (< 20 NTU) and to maximize $Y3$ (> 99%) The parts by weight of $X1$, $X2$ and $X3$ were converted to the percentage by weights before analyzing the result using Statistica® version 10.0 (Stat soft, Inc. USA) and Design Expert® version 8.0 (Stat-Ease, Minneapolis, USA). A best fitted quadratic equation was built for each response Eq. (1).

$$Y = \beta 0 + \beta 1(X1) + \beta 2(X2) + \beta 3(X3) + \beta 11(X1)^2 + \beta 22(X2)^2 + \beta 33(X3)^2 + \beta 12(X1X2) + \beta 13(X1X3) + \beta 23(X2X3) \quad (1)$$

where Y, the response; $\beta 0$, arithmetic means for a particular response; $\beta 1$, $\beta 2$ and $\beta 3$ are the regression coefficient for factor $X1$, $X2$ and $X3$ respectively. A positive coefficient indicates a synergistic effect, while a negative one represents an antagonistic effect. ANOVA was employed to validate these models. Model adequacy tested by inspection of residual plots. The optimum SNEDDS preconcentrate composition was determined using Derringer's desirability function.

2.7. Preparation of liquid SNEDDS

The liquid SNEDDS prepared by dissolving glipizide at 90% SS in optimized SNEDDS preconcentrate. Briefly, 400 mg of glipizide was added to 10 g of SNEDDS preconcentrate and mixed for five minutes with a Cyclo-mixer (CM101, Remi-instruments, Mumbai, India) to get a clear solution.

2.8. Characterization of liquid SNEDDS

2.8.1. Thermodynamic stability studies

Liquid SNEDDS was subjected to thermodynamic stability studies in order to access any phase separation and stability

Table 1 Details of experiments performed along with outcomes during optimization of SNEDDS preconcentrate by a central composite design.

Std. order	Run order	*X*1	*X*2	*X*3	*X*1	*X*2	*X*3	*Y*1		*Y*2		*Y*3	
		By parts (w/w)			By percentage (w/w)			Obs.[a]	Pred.[b]	Obs.[a]	Pred.[b]	Obs.[a]	Pred.[b]
8	1	60.00	60.00	30.00	40.00	40.00	20.00	47.8	30.5	24.3	4.8	99.3	100.8
7	2	20.00	60.00	30.00	18.18	54.54	27.27	42.9	61.3	10.5	22.0	99	95.5
18	3	40.00	40.00	20.00	40.00	40.00	20.00	45.4	48.0	12.2	22.7	99	98.5
10	4	73.63	40.00	20.00	55.10	29.93	14.96	121.1	123.3	175.8	172.8	81	81.3
16	5	40.00	40.00	20.00	40.00	40.00	20.00	49.1	48.0	27.6	22.7	98.2	98.5
4	6	60.00	60.00	10.00	46.15	46.15	7.69	76.6	90.9	112.8	136.3	96.2	93.9
14	7	40.00	40.00	36.81	34.24	34.24	31.51	58.6	55.9	45.8	57.1	97.8	99.5
11	8	40.00	6.364	20.00	60.27	9.58	30.13	158.4	156.9	190.5	186.4	78	78.6
3	9	20.00	60.00	10.00	22.22	66.66	11.11	35.6	18.3	7.5	1.1	99.3	101.4
6	10	60.00	20.00	30.00	54.54	18.18	27.27	105.2	122.7	162.0	173.3	84.8	81.6
17	11	40.00	40.00	20.00	40.00	40.00	20.00	46.5	48.0	19.2	22.7	98.3	98.5
1	12	20.00	20.00	10.00	40.00	40.00	20.00	47.1	64.5	22.5	46.9	98	95.4
12	13	40.00	73.63	20.00	29.93	55.10	14.96	39.5	40.5	9.4	6.2	99	99.7
15	14	40.00	40.00	20.00	40.00	40.00	20.00	49.7	48.0	29.5	22.7	98.7	98.5
20	15	40.00	40.00	20.00	40.00	40.00	20.00	45.8	48.0	14.2	22.7	98.9	98.5
5	16	20.00	20.00	30.00	28.57	28.57	42.85	84.7	70.5	121.8	103.3	95.9	97.1
19	17	40.00	40.00	20.00	40.00	40.00	20.00	51.9	48.0	32.8	22.7	98.7	98.5
9	18	6.36	40.00	20.00	9.58	60.27	30.13	20.9	18.3	4.6	0.3	99.9	100.5
13	19	40.00	40.00	3.18	48.08	48.08	3.82	99.4	101.6	138.7	120.2	92.8	92.4
2	20	60.00	20.00	10.00	66.66	22.22	11.11	238.4	220.1	275.8	269.2	64.8	67.2

*X*1, Captex 355; *X*2, Solutol HS 15; *X*3, Imwitor 988; *Y*1, mean droplet size (nm); *Y*2, turbidity (NTU) and *Y*3, percentage transmittance.
[a] Observed.
[b] Predicted.

of the formed nanoemulsion (Bandyopadhyay et al., 2012; Shakeel et al., 2013).

2.8.1.1. Centrifugation test. Liquid SNEDDS was diluted 500 times with water (HPLC). Two ml of the diluted portion centrifuged at 5000 rpm (RM 12C, Remi, Mumbai, India) for 30 min and was observed visually for any sign of phase separation.

2.8.1.2. Heating and cooling cycle. Liquid SNEDDS was subjected to six cycles of heating (40 °C) and cooling (4 °C) with 48 h storage at each temperature. Afterward, it was assessed for phase separation.

2.8.2. Cloud point measurement

Liquid SNEDDS was diluted 500 times with water (HPLC) and placed into a water bath, and the temperature increased gradually. The temperature at which a sudden appearance of turbidity occurs was recorded. This was verified by measuring turbidity using a Nephlo-turbidity meter (132, Systronics, India) (Bandyopadhyay et al., 2012).

2.8.3. Measurement of droplet size analysis and zeta potential

0.1 g of liquid SNEDDS was diluted with 50 ml of water (HPLC) in a volumetric flask. The flask was inverted and shaken gently to form a fine emulsion and allowed to stand for 12 h at room temperature (Balakrishnan et al., 2009). The droplet size and zeta potential of the diluted liquid SNEDDS was determined using dynamic light scattering (DLS) techniques with a particle sizer (Nanopartica SZ100, Horiba instrument, UK).

2.8.4. Measurement of transmittance and turbidity

The percentage transmittance and turbidity of the formed emulsion in Section 2.8.3 were measured using UV–Vis spectrophotometer (T80+, PG Instrument, UK) and Digital Nephlo-turbidity meter (132, Systronics, India) respectively using water (HPLC) as blank.

2.8.5. Transmission electron microscopy

The morphology of the formed nanoemulsion in Section 2.8.3 was determined using transmission electron microscopy (TEM) (JEM-1200EX, Jeol, Japan). A drop of diluted liquid SNEDDS spread on a 200-mesh, copper grid and positively stained with 0.5% uranyl acetate for 30 s. The grid dried at room temperature and then observed using TEM.

2.9. Preparation of solid SNEDDS and determining drug content

Liquid SNEDDS was adsorbed onto a popular inorganic adsorbent such as Calcium carbonate (Tang et al., 2008). Briefly, 10 g of liquid SNEDDS (obtained in Section 2.7) was poured onto calcium carbonate (15 g) placed in a mortar, mixed for five minutes to obtain a homogenous mass. 2 g of Talc (used as lubricant) was added to the above mass, mixed gently, and passed through a 250 µm mesh. Similarly, a solid SNEDDS blank prepared using above excipients in the same proportion but without using glipizide.

For determining drug content, the 100 mg of solid SNEDDS was transferred into 10 ml volumetric flask, and the volume made up to mark with methanol (HPLC) and sonicated for 10 min. Two ml of the above solution was diluted

to 10 ml with mobile phase, mixed, filtered through a 0.22 μm nylon filter, and injected six times into the HPLC system. Similarly, blank injections were made in the same way by using solid SNEDDS blanks. The amount of solid SNEDDS equivalent to 5 mg of glipizide was filled into size "1" hard gelatin capsules (Capsugel, Mumbai, India) and stored at 25 °C until used for the subsequent studies.

2.10. Characterization of solid SNEDDS

2.10.1. Droplet size of reconstituted solid SNEDDS

Content of one capsule of Solid SNEDDS was reconstituted in 50 ml of water (HPLC), allowed to stand for 12 h at room temperature and the droplet size was of formed emulsion was measured as per the procedure stated under liquid SNEDDS (Section 2.8.3).

2.10.2. Micromeritic properties

Important micromeritic properties such as Carr's index, Hausner's ratio, and angle of repose of solid SNEDDS were determined using the standard procedure (Carr, 1965).

2.10.3. Scanning electron microscopy (SEM)

The outer macroscopic structures of glipizide, solid SNEDDS, solid SNEDDS blank, and physical mixtures (1:1 mixture of glipizide and solid SNEDDS blank) were investigated by S-4100 scanning electron microscope (Hitachi, Japan) at an accelerating voltage of 15 keV.

2.10.4. Powder XRD studies

X-ray powder scattering measurements on the samples (mentioned in Section 2.10.3) and individual excipients of solid SNEDDS (e.g. Calcium carbonate and Talc) were carried out with an X-ray diffractometer (D8 Advanced, Bruker AXS, Germany). The instrument uses Cu Kα radiation generated at 40 kV voltage and 40 mA current. The 2θ angle increased at a step of 0.1° within 6–50°.

2.10.5. Differential scanning calorimetry (DSC)

DSC analysis of the samples mentioned in Section 2.10.4 was carried out using Pyris 6 DSC thermal analyzers (Perkin Elmer, USA). Samples were scanned at a temperature increment of 10 °C/min from 40 to 320 °C.

2.10.6. In-vitro dissolution studies

In-vitro dissolution studies were conducted for the solid SNEDDS, liquid SNEDDS, marketed product (Glucotrol®, Pfizer Inc. USA) and pure drug each containing 5 mg of glipizide. Studies conducted using a USP dissolution type-I apparatus (TDT-08L, Electrolab, Mumbai, India) with 900 ml of pH 6.8 phosphate buffer as the dissolution medium maintained at 37 ± 0.5 °C. The basket speed was adjusted to 75 rpm. At a predetermined time interval, an aliquot (five ml) of the samples were collected and replaced with fresh dissolution medium. The collected samples were suitably diluted with mobile phase, filtered through 0.22 μm membrane filter and analyzed for the glipizide content by HPLC.

3. Results and discussion

3.1. Solubility study of glipizide and selection of oil

The oil, which is an important excipients in the self-emulsifying formulation enhances solubility and fraction of lipophilic drugs transported through the intestinal lymphatic system, thus increasing absorption through the GI tract (Gursoy and Benita, 2004). The drug loading capability is the main factor needs to be considered during the screening of the oily phase for a self-emulsifying formulation (Pouton, 2000). The saturation solubility of glipizide in LCT such as Coconut oil, Olive oil and Castor oil was found to be 1.35 ± 0.05, 1.28 ± 0.04 and 2.11 ± 0.15 mg/ml respectively. The solubilities of glipizide in MCT such as Captex 300, Captex 355, Labrafac lipophile WL1349, Labrafac PG and Miglyol 812 N were found to be 5.12 ± 0.14, 5.55 ± 0.14, 4.45 ± 0.21, 4.08 ± 0.15 and 4.89 ± 0.22 mg/ml respectively. Solubility of glipizide was found to be much higher in MCT than LCT. This may be due to the shorter chain length and better fluidity of MCT over LCT (Bandyopadhyay et al., 2012). In addition, MCT are easy to nanoemulsify as compared to LCT (Date et al., 2010). Thus, Captex 355 was selected as the oily phase owing to its higher solubilization capacity.

3.2. Screening of surfactant for emulsifying ability

The surfactant forms a thin film at the interface, decreases the globule size, helps in stabilization of the emulsion and exerts their absorption enhancing effect by partitioning into the cell membrane to disrupt the structural organization of the lipid bilayer leading to permeation enhancement (Gursoy and Benita, 2004). Only hydrophilic surfactants (HLB > 12) were screened, as this will favor the formation of oil-in-water emulsion (Mohsin et al., 2009; Pouton, 2000). Only non-ionic surfactants were employed during this study because of less toxicity as compared to the ionic one (Bali et al., 2011). The results for surfactant screening were presented in supplementary table (Table S1). Out of all the surfactants screened, only Cremophor RH40, Solutol HS15 and Labrasol were found to possess good emulsifying abilities. Out of these, Solutol HS15 and Labrasol formed a spontaneous dispersion as compared to Cremophor RH40, where the dispersion passed through a noticeable intermediate crystalline phase. Among Solutol HS15 and Labrasol, the dispersion obtained in case of Solutol HS15 was associated with a lower turbidity (102.5 NTU) and higher transmittance (94.1%) as compared to labrasol (296.6 NTU, and 82.5% transmittance). In case of rest surfactants such as Cremophor EL and Tween 80, the resulting dispersion formed a crystalline gel that was difficult to disperse. Solutol HS15 was selected for further study, due to its good dispersibility ability. Solutol HS15 with an average HLB of 15 has an inhibitory effect on p-gp enzymes, thus increases intestinal absorption of drugs (Cornaire et al., 2004). Solutol HS15 was reported to improve bioavailability of some drugs formulated as self-emulsifying formulations, such as Progesterone (Abdalla et al., 2008), Cefpodoxime proxetil (Date and Nagarsenker, 2007), Dipyridamole (Guo et al., 2011).

3.3. Screening of co-surfactant for emulsifying ability

The co-surfactant penetrates into the interface causing void spaces for water penetration. This increases interfacial fluidity that facilitates spontaneous formation of emulsion (Nazzal and Khan, 2002). The results for co-surfactant screening were shown in supplementary table (Table S2). Imwitor 988 showed the highest emulsifying ability as the dispersion obtained from Imwitor 988 was found to be associated with a higher transmittance (97.5%) along with lower turbidity (74.3 NTU) as compared to the rest co-surfactant such as Capmul MCM (97.1%, 78.6 NTU), Capmul PG 8 (93.6%, 151.1 NTU), and PEG 400 (92.5%, 174.5 NTU). The results clearly indicated that lipophilic co-surfactant like Imwitor 988, and Capmul MCM possesses better emulsifying ability than hydrophilic co-surfactant such as PEG 400 and Capmul PG8, which contains hydrophilic glycol moieties. Lipophilic co-surfactant, possesses a better miscibility ability with MCT, has better ability to promote emulsification, has good solvent capacity for drugs and lack of susceptibility to oxidation and hydrolysis compared to hydrophilic co-surfactant (Pouton and Porter, 2008). Imwitor 988, having a short Caprylic acid (C8) back bone was selected for the study due to a better emulsifying ability than Capmul MCM (a mixture of C8 and C10 fatty acids). Co-surfactant with a shorter molecular chain length is considered to be more efficient and has better ability to promote water penetration (Date and Nagarsenker, 2007).

3.4. Ternary phase diagram

Ternary phase diagram was constructed in an absence of the drug to identify the self-nanoemulsifying regions. Ternary phase diagram was plotted for the selected oil (Captex 355), surfactant (Solutol HS15) and co-surfactant (Imwitor 988) being each of them at the apex of a triangle (Gupta et al., 2011) is shown in supplementary figure (Fig. S1). It was observed that either a high or low concentration of oil, surfactant and co-surfactant resulted in a turbid emulsion. The region of a clear or slightly bluish dispersion (nanoemulsion region) was appeared between the combination of Captex 355 (20–60% w/w), Solutol HS15 (20–60% w/w) and Imwitor 988 (10–30% w/w).

3.5. Optimization of SNEDDS preconcentrate using experimental design

Following ternary phase diagram studies, a circumscribed CCD ($\alpha = 1.682$) was employed for the systematic optimization of the SNEDDS. The self-emulsifying formulations of Sirolimus (Hu et al., 2012) and Baicalein (Liu et al., 2012) have been optimized by circumscribed CCD. The ranges for oil, surfactant and co-surfactant for CCD based on the ranges as obtained in phase diagram studies. In the present study, to test self-nanoemulsification efficiency of SNEDDS, water (HPLC) used as dispersion media because a non-significant difference in droplet size has been observed if SNEDDS dispersed in either water or GI fluids (Shakeel et al., 2013).

3.5.1. Influence of factors on droplet size (nm)

The droplet size of the emulsion is a crucial factor in self-emulsification performance because it determines the rate and extent of drug release as well as absorption (Pouton, 2006). As it can be seen from Fig. 1a and b, an increase in % w/w of Captex 355 tends to increase the droplet size where as a reversed pattern was observed with Solutol HS15. The droplet size was decreased with an increasing % w/w of Imwitor 988

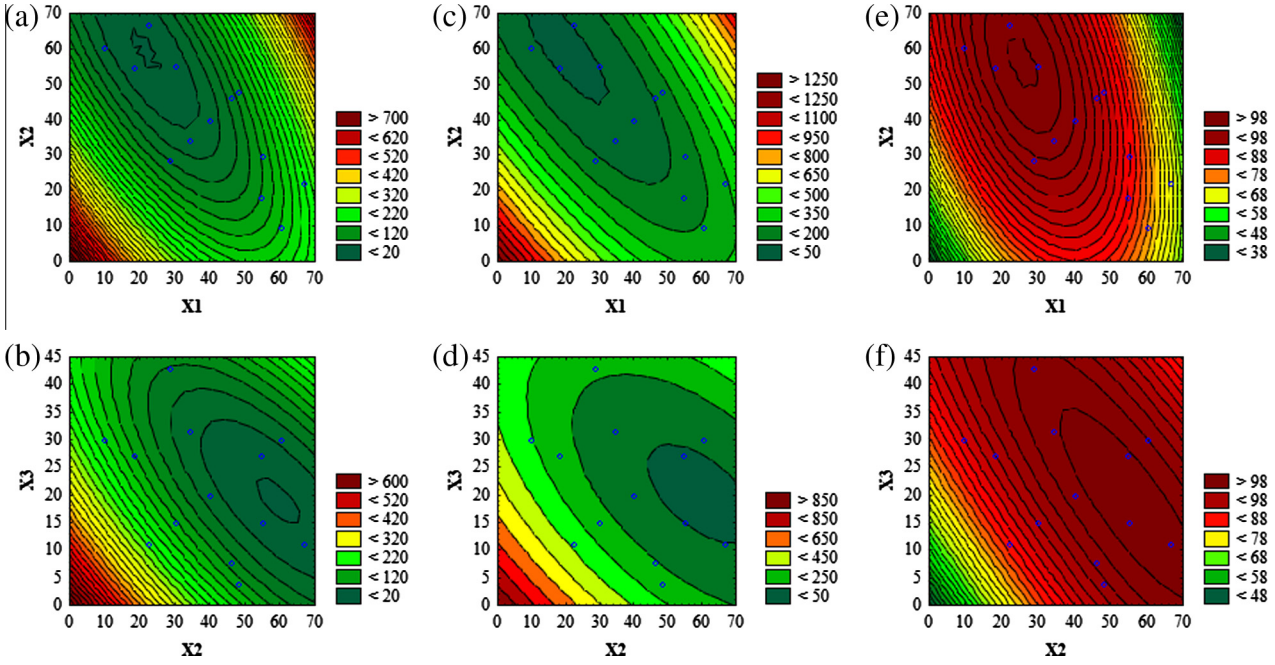

Figure 1 Contour plots (a and b) for mean droplet size (nm); (c and d) for NTU and (e and f) for percentage transmittance. Where; *X*1, percentage (w/w) of Captex 355; *X*2, percentage (w/w) of Solutol HS15 and *X*3, percentage (w/w) of Imwitor 988. The small blue circle represents actual data points.

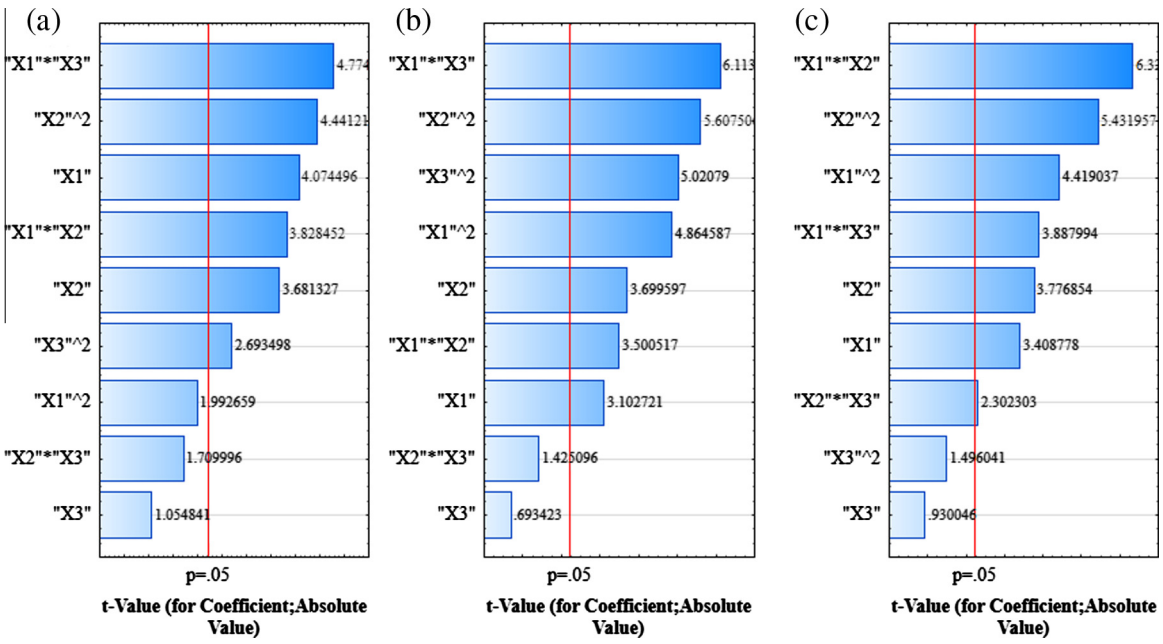

Figure 2 Pareto charts for mean droplet size (nm) (a), NTU (b) and percentage transmittance (c). Where; $X1$, percentage (w/w) of Captex 355; $X2$, percentage (w/w) of Solutol HS15 and $X3$, percentage (w/w) of Imwitor 988.

(Fig. 1b). The regression equation obtained for droplet size ($Y1$) is as below Eq. (2).

$$Y1 = 80.0416 + 4.6121(X1) - 4.167(X2) - 2.388(X3) + 0.0201(X1)^2 + 0.0448(X2)^2 + 0.1087(X3)^2 - 0.0518(X1 \cdot X2) - 0.1293(X1 \cdot X3) + 0.0463(X2 \cdot X3) \quad (2)$$

The mean droplet size of diluted SNEDDS preconcentrates were found to be between 20.9 nm and 238.4 nm (Table 1). Pareto analysis of droplet size (Fig. 2a) shows the significant linear ($X1$) effect of Captex 355 ($p < 0.05$; Table 2), where the coefficient was found to be positive (Eq. (2)). This implies that, an increase in Captex 355 leads to an increase in droplet size. Whereas, the quadratic effect of Captex 355 $(X1)^2$ was found to be non-significant ($p > 0.05$), indicating an absence of any abrupt increase in droplet size with a gradual increase in Captex 355 concentrations. An increase in Captex 355, a hydrophobic MCT increases surface tension at the oil water interface that proceeds through a liquid crystalline phase leading to coarser and aggregated droplet (Pouton and Porter, 2008). The linear ($X2$) effect of Solutol HS15 was found to be significant ($p < 0.05$; Table 2) with a negative coefficient (Eq. (2)), indicating a decrease in droplet size. This may be attributed to the surface tension lowering property of surfactant at the oil water interface that lessens the free energy required for the formation of finer emulsion (Gursoy and Benita, 2004). A significant ($p < 0.05$, Table 2) negative interaction (decrease in droplet size) was observed between Captex 355 and Solutol HS15 ($X1X2$), signifying Solutol HS15 successfully counteracted the increase in interfacial surface tension caused by Captex 355. This in turn decreased the droplet size. In contrast, the quadratic effect of Solutol HS15 $(X2)^2$ was found to be significant ($p < 0.05$; Table 2) having a positive coefficient (an increase in droplet size) (Coefficient: +0.0448, Eq. (2)). This might be due to an enhanced water penetration into the oil droplets mediated by excess surfactant concentration causing disruption of interfacial surface and led to the ejection of oil droplets into the aqueous phase, which in turn forms a coarse emulsion having larger droplet size (Gursoy and Benita, 2004). The linear effect of Imwitor 988 ($X3$) was found to be non-significant ($p > 0.05$; Table 2) indicating co-surfactant by itself does not possess emulsifying ability; rather it acts by enhancing water penetration and interfacial fluidity (Pouton and Porter, 2008). This phenomenon was verified by a significant ($p < 0.05$; Table 2) negative interaction that observed between Captex 355 and Imwitor 988 ($X1X3$), which indicate the ability of Imwitor 988 to counteract the effect of Captex 355 and providing more flexibility for the rupture of liquid crystalline phase to enhance water penetration. And this interactive effect ($X1X3$) had the most profound effect upon droplet size owing to its highest F value (22.80, Table 2) and the longest bar length as shown in Pareto chart (Fig. 2a). A significant ($p < 0.05$; Table 2) interaction bearing positive coefficient (+0.0463, Eq. (2)) (an increase in droplet size) was observed between Solutol HS15 and Imwitor 988 ($X2X3$). This may be due to an additive water penetrating effect of surfactant and co-surfactant causing disruption of interfacial surface leading to ejection of oil droplets into the aqueous phase. The average difference between predicted and experimental mean droplet size was approximately 8.0 nm and the largest difference was 18.4 nm.

3.5.2. Influence of factors on turbidity (NTU)

Turbidity can be used as an indirect measure of emulsion droplet size as a direct correlation been observed between the intensity of scattered light and the volume of dispersed droplets (Nazzal and Khan, 2002). From the contour plot (Fig. 1c), it was found that the turbidity was decreased gradually with an increase (up to 50% w/w) in Captex 355. Turbidity was increased with a further increase in % w/w of Captex 355. Turbidity was found to be decreased with an

Table 2 Analysis of variance (ANOVA) of models.

Source	DF [a]	*Y*1		*Y*2		*Y*3	
		F[b]	p[c]	*F*[b]	*p*[c]	*F*[b]	*p*[c]
Regression	9	22.68	< 0.001*	41.82	< 0.001*	33.36	< 0.001*
Linear	3	14.43	0.001*	10.87	0.002*	12.24	0.001*
*X*1	1	16.60	0.002*	9.63	0.011*	11.62	0.007*
*X*2	1	13.55	0.004*	13.69	0.004*	14.26	0.004*
*X*3	1	1.11	0.316	0.48	0.504	0.86	0.374
Square	3	8.90	0.004*	22.36	< 0.001*	15.03	< 0.001*
*X*1**X*1	1	3.97	0.074	23.66	0.001*	19.53	0.001*
*X*2**X*2	1	19.72	0.001*	31.44	< 0.001*	29.51	< 0.001*
*X*3**X*3	1	7.25	0.023*	25.21	0.001*	2.24	0.166
Interaction	3	13.46	0.001*	17.22	< 0.001*	20.15	< 0.001*
*X*1**X*2	1	14.66	0.003*	12.25	0.006*	40.04	< 0.001*
*X*1**X*3	1	22.80	0.001*	37.38	< 0.001*	15.12	0.003*
*X*2**X*3	1	2.92	0.118	2.03	0.185	5.30	0.044*
Lack-of-fit	5	1.25	0.293	0.69	0.425	0.82	0.382

*X*1, Captex 355; *X*2, Solutol HS 15 and *X*3, Imwitor 988; *Y*1, mean droplet size (nm); *Y*2, turbidity (NTU); *Y*3, percentage transmittance.
[a] DF, degree of freedom.
[b] *F*, test for comparing model variance with residual variance.
[c] *p*, probability of seeing the observed *F*-value if the null hypothesis is true.
* Significant model terms ($p < 0.05$).

increased % w/w of Solutol HS15 and Imwitor 988 (Fig. 1c-d). The regression equation for turbidity (*Y*2) is as below in Eq. (3).

$$Y2 = 77.4078 + 4.0379(X1) - 4.8147(X2) - 1.8048(X3) + 0.0564(X1)^2 + 0.065(X2)^2 + 0.233(X3)^2 - 0.0545(X1 \cdot X2) - 0.1904(X1 \cdot X3) - 0.0444(X2 \cdot X3) \quad (3)$$

The observed turbidities of the diluted SNEDDS preconcentrates were found to be within 4.6–275.8 NTU (Table 1). It can be concluded from Pareto chart (Fig. 2b) and ANOVA (Table 2), that all the model terms, except *X*3 and *X*2*X*3 were found to be significant ($p < 0.05$; Table 2). A significant ($p < 0.05$; Table 2) negative interaction (a decrease in turbidity) was observed between Captex 355 and Solutol HS15 as well as between Captex 355 and Imwitor 988. The later was found to be the most significant one affecting turbidity due to its highest F value (37.38, Table 2). The average and largest difference between observed and predicted turbidity was found to be 10.5 NTU and 24.4 NTU respectively. The results indicated that, the significance as well as the direction of these effects upon turbidity (*Y*2) was similar to the effects as observed upon droplet size (*Y*1) except the quadratic effect of Captex 355 $(X1)^2$. $(X1)^2$ had a significant ($p < 0.05$) effect upon turbidity whereas its effect upon the droplet size was non-significant ($p > 0.05$). A good correlation ($r^2 = 0.919$) was observed between turbidity and droplet size.

3.5.3. Influence of factors on percentage transmittance

A value of percentage transmittance closer to 100% indicates that the dispersion of SNEDDS was clear and transparent with a droplet size that approximates the nanometer range. This in turn provides a large surface area for the drug release and absorption in the GI tract (Bali et al., 2011). From Fig. 1e, it can be observed that, initially percentage transmittance increased by an increase in Captex 355 (up to 50% w/w). However, percentage transmittance was decreased with a further increase in % w/w of Captex 355. Percentage transmittance was increased by an increasing % w/w of Solutol HS15 and Imwitor 988 (Fig. 1e and f). The regression equation obtained for percentage transmittance is as follows Eq. (4).

$$Y3 = 91.4713 - 0.584(X1) + 0.6471(X2) + 0.3187(X3) - 0.0067(X1)^2 - 0.0083(X2)^2 - 0.0091(X3)^2 + 0.013(X1 \cdot X2) + 0.0159(X1 \cdot X3) - 0.0094(X2 \cdot X3) \quad (4)$$

The range of percentage obtained after diluting SNEDDS preconcentrates varied between 64.8% and 99.9% (Table 1). It can be seen from the Pareto chart (Fig. 2c), that all the model terms except linear (*X*3) and quadratic $(X3)^2$ effects of Imwitor 988 were found to be significant ($p < 0.05$; Table 2). Significant ($p < 0.05$; Table 2) positive interaction was observed between Captex 355 and Solutol HS15 (*X*1*X*2) as well as between Captex 355 and Imwitor 988 (*X*1*X*3). A significant ($p < 0.05$; Table 2) negative interaction (a decrease in percentage transmittance, unfavorable) was observed between Solutol HS15 and Imwitor 988 (*X*2*X*3). Out of all the model terms, *X*1*X*2 had the most profound effect upon percentage transmittance owing to its highest bar length as observed in Pareto chart (Fig. 2c) and highest F value (40.04, Table 2). The average difference between observed and predicted transmittance was 1.24% and the largest difference was 3.5%. From these results, it can be clearly observed that the effects of factors upon percentage transmittance (*Y*3) were very similar to the effects as observed upon the droplet size but in an opposite direction. A good correlation ($r^2 = 0.946$) between percentage transmittance and droplet size was observed. Thus, this study supports the previous works, those employ percentage transmittance as one of the quality parameters for characterization of SNEDDS (Bali et al., 2010, 2011; Rahman et al., 2012). Hence, the measurement of percentage transmittance and turbidity of diluted SNEDDS by simpler equipment could be alternative techniques rather than measuring droplet size by expensive and sophisticated equipment.

3.5.4. Validation and adequacies of the models

The ANOVA Result (Table 2) depicts a high F value (22.68 for *Y*1, 41.82 for *Y*2 and 33.36 for *Y*3) along with a low "*p*" value ($p < 0.001$). In addition, it can be observed from Table 2, that the lack of fits were found to be non-significant ($p > 0.05$) for each model, indicating that the proposed models are appropriate and significant. The relationships between observed and predicted responses was found to be linear and acceptable as the adjusted R^2 values were higher than 0.8 (0.9112 for *Y*1, 0.9508 for *Y*2 and 9387 for *Y*3) as suggested by Lundstedt et al., 1998 for chemical samples. Residuals for all responses were found to be homogenous, structure less and having an independence pattern that distributed equally above and below 0-line. The residuals were normally distributed and resembled a straight line for each response. This implies that the proposed models are adequate, and the variance of the experimental measurements is constant at all values of responses (Montgomery, 2013).

3.5.5. Derringer's desirability and optimization of SNEDDS

The aim of this optimization was set to determine the levels of the factors from which SNEDDS with high-quality characteristics may be produced. As per the method goal, some of the responses desired to be minimized such as droplet size (< 50 nm) and turbidity (< 20 NTU), whereas at the same time some response such as percentage transmittance desired to be maximized (> 99%). Under these conditions, the desirability (*d*) of each of the responses can be combined to get global desirability (d_G) that can be employed to get an optimum combination of factors (Derringer and Suich, 1980). d_G can be represented as Eq. (5).

$$dG = [d1^{p1} x d2^{p2} x \ldots x \cdot dn^{pn}]^{1/n} \quad (5)$$

where the dimensionless term "*d*" (Derringer's desirability function) varies between 0 (undesirable) and 1 (fully desirable), $d_1 \ldots d_n$ is the individual desirability for $1 \ldots n$ number of responses; *p* is the weight of the responses. A value of d_G (1 or closer to 1) is required for getting perfect target values for factors. The goal used for droplet size (nm) and turbidity (NTU) minimized and maximized for percentage transmittance. The weight of the responses (*p*) was set equal to 1. The global desirability was found to be 0.99, which is very close to 1 for the optimal SNEDDS consisted of Captex 355 (30% w/w), Solutol HS15 (45% w/w) and Imwitor 988 (25% w/w).

3.6. Solubility of glipizide in optimized SNEDDS and loading of glipizide

Conventionally, the drug loading in SNEDDS is based on the solubility in oil phase rather than the drug solubility in SNEDDS preconcentrate (a mixture of oil, surfactant and co-surfactant). However, to improve the drug loading capacity of SNEDDS, some studies loaded the drug in between 75% and 200% SS in SNEDDS preconcentrate (Pund et al., 2014; Shakeel et al., 2013; Thomas et al., 2013, 2012). Saturation solubility of glipizide in optimized SNEDDS preconcentrate and water was found to be 45.12 ± 1.36 mg/ml, and 0.033 ± 0.0021 mg/ml respectively. The result indicates a significant ($p < 0.001$) enhancement in glipizide solubility (1367-fold) occurred in optimized SNEDDS preconcentrate as compared to its aqueous solubility. However, in order to solubilize glipizide within a short mix-up time, it was loaded at 90% *SS* level (~40 mg/ml) in the optimized SNEDDS preconcentrate.

3.7. Characterization of liquid SNEDDS

3.7.1. Thermodynamic stability studies

Nanoemulsion is the thermodynamically stable systems without phase separation, creaming and cracking, which differentiate it from the micro-emulsion. Thermodynamic stability studies have a vital importance in developing self-emulsifying formulation as a phase separation can be observed in case of unstable formulation (Rahman et al., 2012). Hence, the SNEDDS examined for centrifugation, and heating–cooling cycle, passed these tests as no phase separation, creaming and cracking were observed.

3.7.2. Cloud point measurement

Estimation of cloud point is an important factor for the stability of self-emulsifying formulation. The cloud point is the temperature above which dehydration of self-emulsifying ingredients occurs and turns a clear dispersion to a cloudy one which in turn may affect drug absorption (Gupta et al., 2011). Hence, cloud point of self-emulsifying formulation should be above body temperature (37 °C). The cloud point of SNEDDS was found to be 74 °C, indicating the formed nanoemulsion at the physiological temperature will be a stable one.

3.7.3. Droplet size analysis and zeta potential analysis

Fig. 3a depicts the mean droplet size along with a size distribution of liquid SNEDDS. The mean droplet size was found to be 29.4 nm. The zeta potential of the liquid SNEDDS was found to be −35.0 mV. The negative value of zeta potential may be due to the presence of free fatty acids. A Negative value to the zeta potential of the optimized formulations indicated that the formulations were negatively charged, and sufficient repulsion among emulsion droplets existed to form an un-coagulated system and therefore, gives an indication of a stable system (Parmar et al., 2011).

3.7.4. Measurement of transmittance and turbidity

The turbidity and transmittance of the diluted liquid SNEDDS were found to 6.7 ± 0.1 NTU and 99.7 ± 0.01% respectively ($n = 3$).

3.7.5. Transmission electron microscopy

TEM image of diluted SNEDDS is shown in Fig. 3b. The nanoemulsion droplets were appeared to be un-coagulated and spherical with a dark background. The droplet size was found to be below 100 nm, having size distribution similar to the result as obtained by DLS technique.

3.8. Characterization of solid SNEDDS

3.8.1. Droplet size of reconstitute solid SNEDDS

The mean droplet size of reconstituted solid SNEDDS was found to be 29.8 and was non-significant ($p > 0.05$) when compared to the droplet size as observed in case of liquid

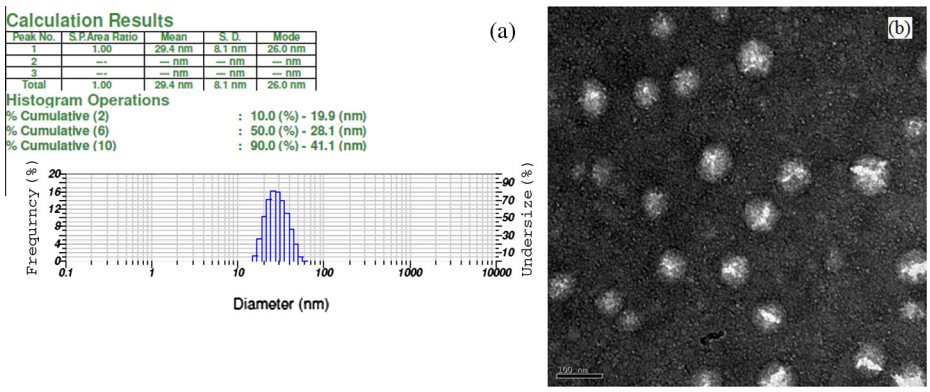

Figure 3 (a) Dynamic light scattering data of the diluted liquid SNEDDS (500 times with HPLC water); (b) transmission electron microscope image of the diluted liquid SNEDDS (500 times with HPLC water), bar length represents 100 nm.

SNEDDS. Hence, solid SNEDDS preserved the selfemulsification property of liquid SNEDDS.

3.8.2. Micromeritic properties

Solid SNEDDS showed a good flow property with Carr's index between 18 and 20, Hausner's ratio within 1.22–1.25 and angle of repose between 25° and 30°.

3.8.3. Scanning electron microscopy (SEM)

The scanning electron micrographs of glipizide, solid SNEDDS, solid SNEDDS blank and physical mixtures were shown in Fig. 4. Glipizide (Fig. 4a) appeared as smooth surfaced rectangular crystals, which can be seen in the physical mixture (Fig. 4d). Whereas glipizide crystals were absent in solid SNEDDS (Fig. 4b), the surface of which was found to be in close resemblance with the agglomerated and rough surfaced solid SNEDDS blank (Fig. 4c). This suggests that the glipizide was absorbed and molecularly dissolved inside the pores of the excipient's matrix of solid SNEDDS. The microporous surface of the matrix might form channels for water infiltration, which could facilitate dispersion and formation of nanoemulsion as suggested by Hu et al., 2012.

3.8.4. Powder XRD studies

X-ray diffractogram of glipizide (Fig. 5a) exhibited several sharp peaks at 7.4°, 10.0°, 11.0°, 15.7°, 16.9°, 18.0°, 18.7°, 19.2°, 20.5°, 21.0°, 21.8°, 22.2°, 23.6°, 24.3°, 24.7°, 25.3°, 26.8° and 28.7° respectively. This was found to be similar to the one reported earlier by Huang et al., 2013. The high-intensity peaks due to glipizide and each excipient were seen in the physical mixture (Fig. 5b). Calcium carbonate showed sharp peaks at 19.2°, 19.7°, 20.1° and 29.5° (Fig. 5e). Talc showed sharp peaks at 9.5°, 19.1°, 19.5°, 28.7° and 36.4° (Fig. 5f). These peaks of calcium carbonate and talc were appeared in solid SNEDDS blank (Fig. 5d), solid SNEDDS (Fig. 5c) and physical mixture (Fig. 5b). In case of solid SNEDDS

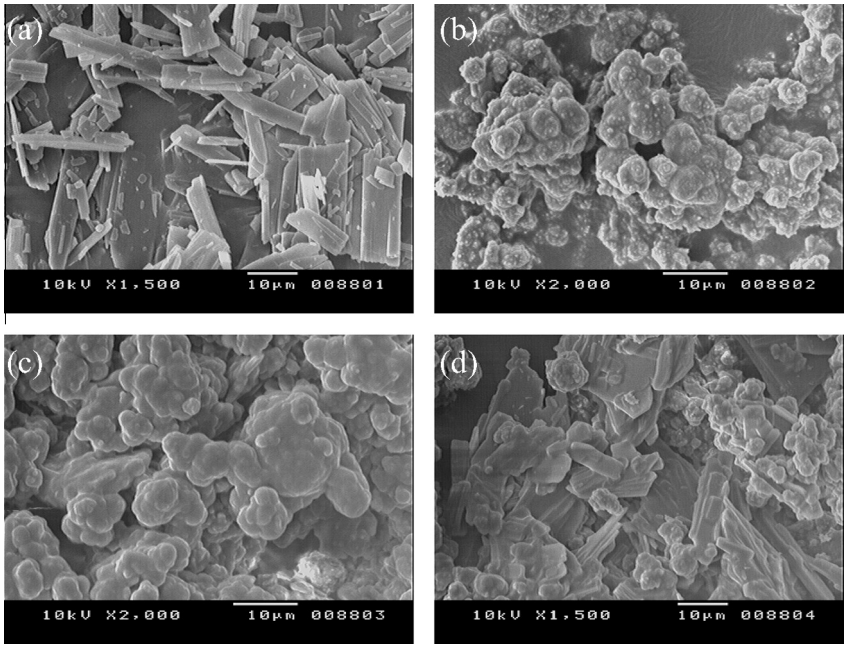

Figure 4 Scanning electron micrograph of: (a) glipizide; (b) solid SNEDDS; (c) solid SNEDDS blank; (d) physical mixture of glipizide and solid SNEDDS blank.

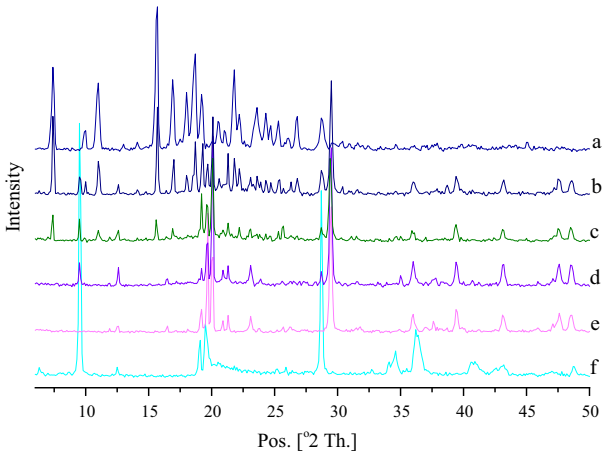

Figure 5 Powdered XRD diffractogram of: (a) glipizide; (b) physical mixture of glipizide and solid SNEDDS blank; (c) solid SNEDDS; (d) solid SNEDDS blank; (e) calcium carbonate and (f) talc.

(Fig. 5c), the major peaks of glipizide (at 7.4°, 11.0°, 15.7°, 16.9° and 22.2°) were found to be of reduced intensity along with a complete absence at 18.0° and 18.7°. This suggests that, the crystalline property of glipizide has been reduced within the solid SNEDDS, where it is present in an amorphous form.

3.8.5. Differential scanning calorimetry (DSC)

DSC thermograms of glipizide, physical mixture, solid SNEDDS, solid SNEDDS blank and excipients were presented in the Fig. 6. It can be observed that, glipizide exhibited a sharp melting endothermic peak at 211.4 °C corresponds to its melting point that initiated from 207.9 °C (Fig. 6a). Physical mixture showed an endothermic peak with reduced intensity relative to the pure glipizide (Fig. 6b). In case of physical mixture, solubilization of glipizide crystals within solid SNEDDS blank during heating might lead to an obtuse peak with reduced intensity. Solid SNEDDS (Fig. 6c) did not show

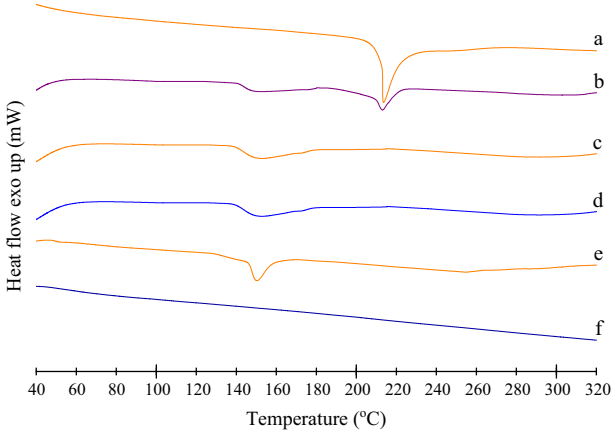

Figure 6 Differential scanning calorimetry (DSC) thermograms of: (a) glipizide; (b) physical mixture of glipizide and solid SNEDDS blank; (c) solid SNEDDS; (d) solid SNEDDS blank; (e) calcium carbonate and (f) talc.

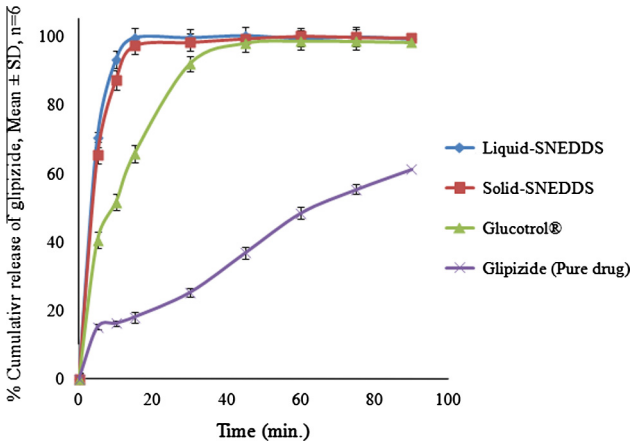

Figure 7 In-vitro release profile of liquid SNEDDS, solid SNEDDS, marketed product (Glucotrol®) and pure drug.

any endothermic peak of glipizide, and its thermogram resembled like thermogram of solid SNEDDS blank (Fig. 6d). Hence, it can be concluded that glipizide was dissolved into the excipient matrix of solid SNEDDS. This has also indicated a change in the physical nature of glipizide from crystalline state to the amorphous one.

3.8.6. In-vitro dissolution studies

In the self-emulsifying systems, the free energy necessary to form an emulsion is very low, thereby allowing the spontaneous formation of the oil/water interface. It is proposed that the oil/surfactant/co-surfactant and water phases effectively swell to decrease the droplet size, and eventually increase the release rate (Balakrishnan et al., 2009). The percentage drug release in 15 min (DR_{15min}) for liquid-SNEDDS, solid-SNEDDS, Glucotrol®, and pure drug was found to be 99.65, 97.33, 65.82, and 18.37 respectively (Fig. 7). This increase in DR_{15min} in case of liquid SNEDDS and solid SNEDDS was significant as compared to Glucotrol® and pure drug. However, the difference observed between DR_{15min} of solid SNEDDS and liquid SNEDDS was found to be non-significant ($p > 0.05$), indicating that the solid SNEDDS preserved the improvement of the *in-vitro* dissolution of liquid SNEDDS. Initially, the glipizide release from solid SNEDDS was marginally slower than its release from liquid SNEDDS, though the difference was statistically non-significant ($p > 0.05$). This could be due to an increase in diffusion path length for the liquid SNEDDS that adsorbed within the porous matrix of solid SNEDDS (Dixit and Nagarsenker, 2008). The superior drug release from solid SNEDDS might be attributed to the presence of amorphous glipizide within as confirmed from PXRD and DSC results. Amorphous form requires less energy to dissolve, resulting in higher apparent solubilities and increased dissolution rates (Seo et al., 2013). In addition, as evident from the SEM results, since glipizide is molecularly dissolved within the solid SNEDDS matrix, a high surface area might have generated to improve wettability and *in-vitro* release of the drug. Furthermore, smaller droplet size of the nanoemulsion generated for reconstituted solid SNEDDS might have generated a larger surface area for rapid drug release.

4. Conclusion

In the present study, the formation of a nanoemulsion following dilution of solid SNEDDS was possible because of careful selection and optimization of excipients. The nanoemulsion was found to possess predetermined quality attributes as specified in the goal. PXRD and DSC studies indicated loss of crystallinity of drug within the solid SNEDDS. This result was verified by the scanning electron microscopy studies, which revealed no evidence of drug precipitation on the surface of the carrier. Solid SNEDDS found to be free flowing in nature, preserved the selfemulsifying property of liquid SNEDDS and showed a significant increase in dissolution of glipizide as compared with pure drug and commercial tablet. However, further pharmacokinetic/pharmacodynamic investigations on animal/human models are needed to exploit the maximum potential of solid SNEDDS for glipizide.

Acknowledgments

Authors are thankful to Abitec Corp., Janesville, USA; BASF SE, Ludwigshafen, Germany; Gattefosse Corp., Saint-Priest, France, and Sasol olefins and surfactants, GmbH, Germany for providing excipients used during this study. Authors are thankful to CCMB, Hyderabad for providing the TEM facility for the study.

Appendix A. Supplementary material

Supplementary data associated with this article can be found, in the online version, at http://dx.doi.org/10.1016/j.jsps.2015.01.024.

References

Abdalla, A., Klein, S., Mäder, K., 2008. A new self-emulsifying drug delivery system (SEDDS) for poorly soluble drugs: characterization, dissolution, in vitro digestion and incorporation into solid pellets. Eur. J. Pharm. Sci. 35, 457–464.

Balakrishnan, P., Lee, B.J., Oh, D.H., Kim, J.O., Hong, M.J., Jee, J.P., Kim, J.A., Yoo, B.K., Woo, J.S., Yong, C.S., Choi, H.G., 2009. Enhanced oral bioavailability of dexibuprofen by a novel solid self-emulsifying drug delivery system (SEDDS). Eur. J. Pharm. Biopharm. 72, 539–545.

Bali, V., Ali, M., Ali, J., 2010. Study of surfactant combinations and development of a novel nanoemulsion for minimising variations in bioavailability of ezetimibe. Colloid Surf B Biointerf. 76, 410–420.

Bali, V., Ali, M., Ali, J., 2011. Nanocarrier for the enhanced bioavailability of a cardiovascular agent: in vitro, pharmacodynamic, pharmacokinetic and stability assessment. Int. J. Pharm. 403, 46–56.

Bandyopadhyay, S., Katare, O.P., Singh, B., 2012. Optimized self nano-emulsifying systems of ezetimibe with enhanced bioavailability potential using long chain and medium chain triglycerides. Colloid Surf B Biointerf. 100, 50–61.

Basalious, E.B., Shawky, N., Badr-Eldin, S.M., 2010. SNEDDS containing bioenhancers for improvement of dissolution and oral absorption of lacidipine. I: Development and optimization. Int. J. Pharm. 391, 203–211.

Carr, R.L., 1965. Evaluating flow properties of solids, chemical engineering. Chem. Eng. 18, 163–168.

Cornaire, G., Woodley, J., Hermann, P., Cloarec, A., Arellano, C., Houin, G., 2004. Impact of excipients on the absorption of P-glycoprotein substrates in vitro and in vivo. Int. J. Pharm. 278, 119–131.

Date, A.A., Desai, N., Dixit, R., Nagarsenker, M., 2010. Self-nanoemulsifying drug delivery systems: formulation insights, applications and advances. Nanomedicine 5, 1595–1616.

Date, A.A., Nagarsenker, M.S., 2007. Design and evaluation of self-nanoemulsifying drug delivery systems (SNEDDS) for cefpodoxime proxetil. Int. J. Pharm. 329, 166–172.

Derringer, G., Suich, R., 1980. Simultaneous optimization of several response variables. J. Qual. Technol. 12, 214–220.

Dixit, R.P., Nagarsenker, M.S., 2008. Self-nanoemulsifying granules of ezetimibe: design, optimization and evaluation. Eur. J. Pharm. Sci. 35, 183–192.

Gan, Y., Pan, W., Wei, M., Zhang, R., 2002. Cyclodextrin complex osmotic tablet for glipizide delivery. Drug Dev. Ind. Pharm. 28, 1015–1021.

Guo, F., Zhong, H., He, J., Xie, B., Liu, F., Xu, H., Liu, M., Xu, C., 2011. Self-microemulsifying drug delivery system for improved oral bioavailability of dipyridamole: preparation and evaluation. Arch. Pharm. Res. 34, 1113–1123.

Gupta, S., Chavhan, S., Sawant, K.K., 2011. Self-nanoemulsifying drug delivery system for adefovir dipivoxil: design, characterization, in vitro and ex vivo evaluation. Colloids Surf., A Physicochem. Eng. Asp. 392, 145–155.

Gursoy, R.N., Benita, S., 2004. Self-emulsifying drug delivery systems (SEDDS) for improved oral delivery of lipophilic drugs. Biomed. Pharmacother. 58, 173–182.

Hu, X., Lin, C., Chen, D., Zhang, J., Liu, Z., Wu, W., Song, H., 2012. Sirolimus solid self-microemulsifying pellets: formulation development, characterization and bioavailability evaluation. Int. J. Pharm. 438, 123–133.

Huang, H., Wu, Z., Qi, X., Zhang, H., Chen, Q., Xing, J., Chen, H., Rui, Y., 2013. Compression-coated tablets of glipizide using hydroxypropylcellulose for zero-order release: in vitro and in vivo evaluation. Int. J. Pharm. 446, 211–218.

Isaac, J., Kaity, S., Ganguly, S., Ghosh, A., 2013. Microwave-induced solid dispersion technology to improve bioavailability of glipizide. J. Pharm. Pharmacol. 65, 219–229.

Kushare, S.S., Gattani, S.G., 2013. Microwave-generated bionanocomposites for solubility and dissolution enhancement of poorly water-soluble drug glipizide: in-vitro and in-vivo studies. J. Pharm. Pharmacol. 65, 79–93.

Liu, W., Tian, R., Hu, W., Jia, Y., Jiang, H., Zhang, J., Zhang, L., 2012. Preparation and evaluation of self-microemulsifying drug delivery system of baicalein. Fitoterapia 83, 1532–1539.

Lundstedt, T., Seifert, E., Abramo, L., Thelin, B., Nystrom, A., Pettersen, J., Bergman, R., 1998. Experimental design and optimization. Chemometr. Intell. Lab. Syst. 42, 3–40.

Madhusudhan, S., Panda, A.K., Parimalakrishnan, S., Manavalan, R., Manna, P.K., 2010. Design, in vitro and in vivo evaluation of glipizide Eudragit microparticles. J. Microencapsul. 27, 281–291.

Mahesh, K.V., Singh, S.K., Gulati, M., 2014. A comparative study of top-down and bottom-up approaches for the preparation of nanosuspensions of glipizide. Powder Technol. 256, 436–449.

Mohsin, K., Long, M.A., Pouton, C.W., 2009. Design of lipid-based formulations for oral administration of poorly water-soluble drugs: precipitation of drug after dispersion of formulations in aqueous solution. J. Pharm. Sci. 98, 3582–3595.

Montgomery, D.C., 2013. Design and Analysis of Experiments, eighth ed. John Wiley & Sons Inc., Hoboken, NJ.

Nazzal, S., Khan, M.A., 2002. Response surface methodology for the optimization of ubiquinone self-nanoemulsified drug delivery system. AAPS PharmSciTech 3, E3.

Nie, S., Zhang, S., Pan, W., Liu, Y., 2011. In vitro and in vivo studies on the complexes of glipizide with water-soluble beta-cyclodextrin-epichlorohydrin polymers. Drug Dev. Ind. Pharm. 37, 606–612.

Parmar, N., Singla, N., Amin, S., Kohli, K., 2011. Study of cosurfactant effect on nanoemulsifying area and development of

lercanidipine loaded (SNEDDS) self nanoemulsifying drug delivery system. Colloid Surf B Biointerf. 86, 327–338.

Pouton, C.W., 2000. Lipid formulations for oral administration of drugs: non-emulsifying, self-emulsifying and 'self-microemulsifying' drug delivery systems. Eur. J. Pharm. Sci. 11 (Suppl 2), S93–S98.

Pouton, C.W., 2006. Formulation of poorly water-soluble drugs for oral administration: physicochemical and physiological issues and the lipid formulation classification system. Eur. J. Pharm. Sci. 29, 278–287.

Pouton, C.W., Porter, C.J., 2008. Formulation of lipid-based delivery systems for oral administration: materials, methods and strategies. Adv. Drug Deliv. Rev. 60, 625–637.

Pund, S., Shete, Y., Jagadale, S., 2014. Multivariate analysis of physicochemical characteristics of lipid based nanoemulsifying cilostazol–quality by design. Colloid Surf B Biointerf. 115, 29–36.

Rahman, M.A., Iqbal, Z., Hussain, A., 2012. Formulation optimization and in vitro characterization of sertraline loaded self-nanoemulsifying drug delivery system (SNEDDS) for oral administration. J. Pharm. Invest. 42, 191–202.

Seedher, N., Kanojia, M., 2009. Co-solvent solubilization of some poorly-soluble antidiabetic drugs. Pharm. Dev. Technol. 14, 185–192.

Seo, Y.G., Kim, D.H., Ramasamy, T., Kim, J.H., Marasini, N., Oh, Y.K., Kim, D.W., Kim, J.K., Yong, C.S., Kim, J.O., Choi, H.G., 2013. Development of docetaxel-loaded solid self-nanoemulsifying drug delivery system (SNEDDS) for enhanced chemotherapeutic effect. Int. J. Pharm. 452, 412–420.

Shakeel, F., Haq, N., El-Badry, M., Alanazi, F.K., Alsarra, I.A., 2013. Ultra fine super self-nanoemulsifying drug delivery system (SNEDDS) enhanced solubility and dissolution of indomethacin. J. Mol. Liq. 180, 89–94.

Shivakumar, H.N., Desai, B.G., Pandya, S., Karki, S.S., 2007. Influence of beta-cyclodextrin complexation on glipizide release from hydroxypropyl methylcellulose matrix tablets. PDA J. Pharm. Sci. Technol. 61, 472–491.

Singh, B., Singh, R., Bandyopadhyay, S., Kapil, R., Garg, B., 2013. Optimized nanoemulsifying systems with enhanced bioavailability of carvedilol. Colloid Surf B Biointerf. 101, 465–474.

Sweetman, S.C., 2009. Martindale: The Complete Drug Reference, 36th ed. Pharmaceutical Press, London, Chicago.

Tang, B., Cheng, G., Gu, J.C., Xu, C.H., 2008. Development of solid self-emulsifying drug delivery systems: preparation techniques and dosage forms. Drug Discov. Today 13, 606–612.

Thomas, N., Holm, R., Garmer, M., Karlsson, J.J., Müllertz, A., Rades, T., 2013. Supersaturated self-nanoemulsifying drug delivery systems (Super-SNEDDS) enhance the bioavailability of the poorly water-soluble drug simvastatin in dogs. AAPS J. 15, 219–227.

Thomas, N., Holm, R., Müllertz, A., Rades, T., 2012. In vitro and in vivo performance of novel supersaturated self-nanoemulsifying drug delivery systems (super-SNEDDS). J. Control. Release 160, 25–32.

Wilson, C.O., Gisvold, O., Block, J.H., Beale, J.M., 2004. Wilson and Gisvold's Textbook of Organic Medicinal and Pharmaceutical Chemistry, 11th ed. Lippincott Williams & Wilkins, Philadelphia.

Wu, H., White, M., Khan, M.A., 2011. Quality-by-Design (QbD): an integrated process analytical technology (PAT) approach for a dynamic pharmaceutical co-precipitation process characterization and process design space development. Int. J. Pharm. 405, 63–78.

Zhang, Y.M., Li, X., Sun, C.S., Chen, C.F., 2008. The study on the preparation and spectroscopic properties of hydroxypropyl-beta-cyclodextrin/glipizide inclusion complex. Guang Pu Xue Yu Guang Pu Fen Xi 28, 711–714.